BMC Medicine

RESEARCH

Open Access

Excessive iron accumulation in the striatum associated with addictive behaviors of medication-overuse headache: a prospective study

Xun Pei[1,2], Xiaoyan Bai[1,2], Xue Zhang[1,2], Zhangxuan Hu[5], Wei Wang[3], Xueyan Zhang[4], Yingkui Zhang[1], Hefei Tang[3], Yaqing Zhang[3], Xueying Yu[3], Ziyu Yuan[3], Peng Zhang[3], Tong Chen[1,2], Yuanbin Zhao[1,2], Xiuqin Jia[4], Qi Yang[4*†], Yonggang Wang[3*†] and Binbin Sui[1,6*†]

Abstract

Background Abnormal iron deposition may be a biomarker for a disrupted central antinociceptive neuronal network, and the relationship between iron deposition and the pathophysiological mechanisms of chronic migraine (CM) with medication overuse (MOH) remains unclear. We investigated iron deposition in the deep gray matter (DGM) of the brain in CM patients with and without MOH using quantitative susceptibility mapping (QSM).

Methods Forty-eight healthy controls (HCs) and 69 CM patients (36 with MOH; 33 without MOH) were recruited. QSM data were acquired using a 3.0 T Magnetic resonance imaging (MRI). Regions of interest (ROI) in the DGM, including the bilateral caudate, putamen, globus pallidus (GP), hippocampus, nucleus accumbens, and amygdala, were segmented from the T1-weighted images (T1WI) of the whole brain of each individual patient using FreeSurfer. QSM images were registered to T1WI. QSM values within each ROI were extracted and compared between CM and HCs, as well as between CM with MOH and CM without MOH. Correlations between QSM values and clinical assessment scale scores were calculated. Receiver operating characteristic (ROC) analysis was used to assess the diagnostic performance of QSM values in these DGM for detecting CM and CM with MOH.

Results Compared to HCs, CM patients exhibited increased iron deposition in the caudate ($p = 0.013$) and putamen ($p < 0.001$). In the CM without MOH group, headache duration correlated positively with iron deposition in the caudate (r = 0.502, $p = 0.010$) and putamen (r = 0.514, $p = 0.009$). CM with MOH patients showed greater iron deposition in the caudate ($p < 0.001$), putamen ($p < 0.001$), and GP ($p = 0.049$) than those without MOH, with medication use frequency correlating positively with iron deposition in the caudate (r = 0.427, $p = 0.023$) and putamen (r = 0.445,

†Qi Yang, Yonggang Wang and Binbin Sui contributed equally to this study.

*Correspondence:
Qi Yang
yangyangqiqi@gmail.com
Yonggang Wang
w100yg@gmail.com
Binbin Sui
reneesui@163.com
Full list of author information is available at the end of the article

$p = 0.018$). ROC curve analysis indicated that the caudate (AUC = 0.736) and putamen (AUC = 0.729) exhibited high sensitivity and specificity in diagnosing CM with MOH.

Conclusions CM patients with MOH had excessive iron deposition in basal ganglia regions, including the caudate, putamen, and GP, which may be related to the medication overuse behavior. Iron deposition in the caudate and putamen may be a potential biomarker for CM with MOH. These findings provide insight into the common pathophysiological mechanisms underlying MOH and potential addiction.

Keywords Iron deposition, Quantitative susceptibility mapping, Medication-overuse headache, Addiction, Chronic migraine

Background

Chronic migraine (CM) is a common disabling neurological disorder defined as having headaches for 15 days or more per month, lasting for more than 3 months [1]. At least 50% of CM patients regularly overuse one or more medications for acute migraine, resulting in a CM diagnosis of medication-overuse headache (MOH) [2]. MOH patients often suffer a greater disease burden, with a per capitacost more than three times that of migraines without medication overuse [3] numerous neuroimaging studies have identified structural, functional, and metabolic abnormalities in CM patients with MOH, including volumetric changes in cortical and subcortical regions like insula, precuneus, periaqueductal gray (PAG), thalamus, and ventral striatum; altered striatal functional connectivity and hypometabolism in the thalamus and insula/ventral striatum [4–6]. These findings suggest potential alterations in the pathophysiological mechanisms of CM with MOH.

Iron plays a crucial role in many biochemical processes within the body and is important for maintaining neurological health [7]. Iron-containing molecules primarily accumulate in the deep gray matter (DGM) due to dysfunctional iron regulatory mechanisms in the brain. This abnormality has been identified as a potential biomarker for various central nervous system diseases, including cerebrovascular disease, neurodegenerative diseases and multiple sclerosis, et al. [8, 9]. Numerous studies have demonstrated the involvement of DGM structures in the pathophysiological mechanisms of migraine [10, 11]. Many have also identified structural and functional abnormalities in the DGM of migraine patients, including hippocampal and thalamic atrophy, increased perfusion in the amygdala, and disruptions in functional networks within the basal ganglia [12–14]. Recent investigations have reported excessive iron deposition within specific deep brain regions of individuals with CM, revealing a significant correlation between such deposition and migraine burden [15].

The role of iron deposition in the DGM of CM patients with MOH has not yet been fully elucidated. It is hypothesized that iron deposition within the DGM of the brain may exhibit abnormal patterns in MOH patients, which may be correlated with medication overuse behavior. Quantitative susceptibility mapping (QSM), a method for evaluating tissue susceptibility, has been applied to quantify iron deposition in a range of neurodegenerative disorders [16–18]. Accurately assessing iron deposition in the DGM of CM with MOH patients could provide evidence for the hypothesis of a correlation between iron deposition and medication overuse. This study was conducted to assess iron deposition in various DGM regions of the brain in CM patients with and without MOH using QSM.

Methods

Participants

Our institutional ethics committee approved this study, and all participants provided written informed consent. Between October 2020 and November 2022, we prospectively enrolled 69 patients diagnosed with CM with (n = 36) and without (n = 33) MOH from Headache Clinic at Beijing Tiantan Hospital, affiliated with Capital Medical University and 48 age- and gender- matched healthy controls (HCs). The patient inclusion criteria were as follows: (1) All diagnoses of CM (with and without MOH) met the criteria of the International Classification of Headache Disorders, 3rd edition (ICHD-3), and all patients had migraines without aura. MOH was classified as a complication of CM, characterized by the frequent overuse of medication for acute headache treatment [19, 20]. Specifically, CM was defined as headache occurring on 15 or more days per month for more than three months, with at least eight days per month meeting the features of migraine headache, while MOH was defined as headache occurring on 15 or more days per month in patients with a pre-existing primary headache disorder due to regular overuse of acute or symptomatic headache medication (on 10 or more or 15 or more days per month, depending on the medication type) for more than three months. The diagnosis of all patients was rigorously conducted by three neurologists (W. Wang, Y. Mei, X. Zhang) with six years of clinical experience in headache disorders and

further verified by a chief neurologist (Y. Wang) with over 20 years of experience in headache disorders. (2) Patients had used no migraine prophylactic medication within the past 3 months. (3) Patients were right-handed. Patient exclusion criteria were (1) migraine with other types of primary headache; (2) use of substances (such as alcohol or nicotine) other than the drugs included in the diagnostic criteria; (3) other neurodegenerative diseases; and (4) poor magnetic resonance imaging (MRI) data quality and an imprecise diagnosis. Inclusion criteria for the HCs were (1) absence of abnormal brain lesions or calcifications on cranial imaging and (2) no prior history or manifestations of neurological or mental illness. (3) right-handed. Exclusion criteria for the HCs were (1) history of mental disorders, head trauma, or central nervous system diseases; (2) contraindications to MRI; (3) inability to provide informed consent. Prior to MRI data acquisition, each CM patient underwent a neuropsychological assessment by two neurologists (Z. Yuan, P. Zhang) with 3 years of clinical experience in headache disorders, and the clinical scales were recorded. Visual analogue scales (VAS) were used to assess headache intensity in migraine patients. The Migraine Disability Assessment Questionnaire (MIDAS) was used to assess migraine-related disability; The Headache Impact Test-6 (HIT-6) was used to assess adverse headache effects. Depression severity, anxiety levels, and sleep quality were evaluated using the Patient Health Questionnaire-9 (PHQ-9), the Generalized Anxiety Disorder Questionnaire-7 (GAD-7) scales, and the Pittsburgh Sleep Quality Index (PSQI) clinical scale. Cognitive function was assessed using the Montreal Cognitive Assessment (MoCA). For CM patients with MOH, the monthly medication frequency and continuous medication duration were recorded.

MRI data acquisition

MRI was performed using a GE 3.0 T MRI system (Signa Premier, GE Healthcare, Waukesha, WI, USA) equipped with a 48-channel head coil. All subjects underwent the same MRI scanning protocol. Three-dimensional (3D) T1-weighted anatomical images (T1WI) were obtained using the magnetization-prepared rapid gradient-echo (MP-RAGE) sequence with 1.0-mm isotropic resolution. The parameters used were repetition time (TR) = 400 ms, echo time (TE) = 3 ms, slice thickness = 1 mm, number of slices = 192, flip angle = 8°, field of view (FOV) = 256 × 256 mm^2, reconstruction matrix = 256 × 256, acceleration factor = 2, and acquisition time = 4 min. The QSM sequence was acquired using a multi-echo 3D gradient recalled echo sequence (GRE) with the following parameters: TE = 4.0/8.9/13.7/18.5/23.4 ms, TR = 27.4 ms, matrix = 240 × 240, slice thickness = 1.8 mm, flip angle = 20°, FOV = 220 × 220 mm^2, and voxel size = 0.9 × 0.9 × 1.8 mm^3. The acquisition time was 2 min and 34 s.

Imaging analysis

QSM preprocessing was based on the QSMbox 2.0 software package (https://gitlab.com/acostaj/QSMbox) [21] implemented in MATLAB (The MathWorks, Natick, MA, USA). First, the phase images were extracted for unwrapping and estimating the local magnetic field. Next, the Laplace boundary value method and variable spherical mean value algorithms were used to remove the background field. The Multi-Scale Dipole Inversion (MSDI) algorithm (https://github.com/fil-physics/Publication-Code) was used to convolve the dipole field with the susceptibility in k-space. Brain extraction was conducted using the Brain Extraction Tool (BET) in the Functional Magnetic Resonance Imaging of the Brain (FMRIB) software library v6.0 (FSL) developed by the University of Oxford, UK (https://fsl.fmrib.ox.ac.uk/fsl/fslwiki/FSL). Regions of the DGM, including the bilateral caudate, putamen, globus pallidus (GP), thalamus, nucleus accumbens, hippocampus, and amygdala [22] (Fig. 1), were segmented on T1WI using the"recon-all"function in FreeSurfer (http://surfer.nmr.mgh.harvard.edu/) [23]. Then, the registration workflow is as follows (Fig. 2). First, T1WI underwent preprocessing steps including brain extraction, bias field correction, and normalization. Then, the magnitude image of the first echo from the GRE sequence was extracted, and brain extraction was performed on this magnitude image. The extracted magnitude image was then registered to the T1WI using FLIRT (Linear Image Alignment Tool for FMRIB) [24], generating a transformation matrix. This matrix was subsequently applied to the QSM map to align it with the T1 image. The registration accuracy was verified by a neuroradiologist (X. Pei) with 3 years of clinical experience. Following initial quality assessment and manual adjustments, all ROI delineations underwent rigorous validation and refinement by a senior neuroradiologist (B. Sui) with 15 years of expertise in quantitative neuroimaging analysis. The average whole-brain QSM value for each participant was used as a susceptibility reference [25].

Statistical analyses

Statistical analyses were conducted using SPSS 25.0 software (SPSS Inc., Chicago, IL, USA). All continuous variables are reported as means ± standard deviation or the median with range, depending on whether they followed a normal distribution. Categorical variables are presented as percentages and analyzed using the chi-square test or Fisher's exact test. Independent T-tests or Mann–Whitney U-tests were employed to compare QSM values and other continuous variables.

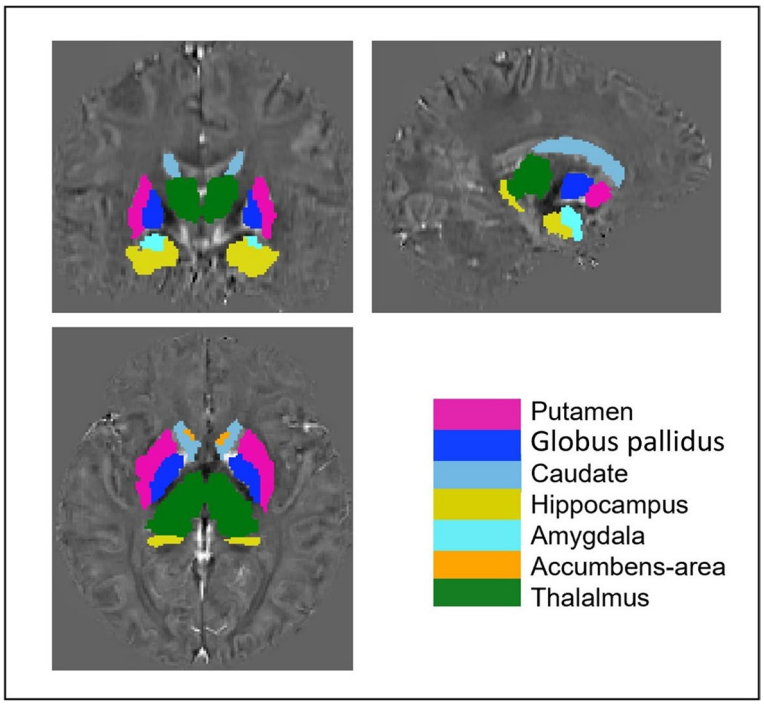

Fig. 1 Position of DGM in the axial, sagittal and coronal sections on QSM

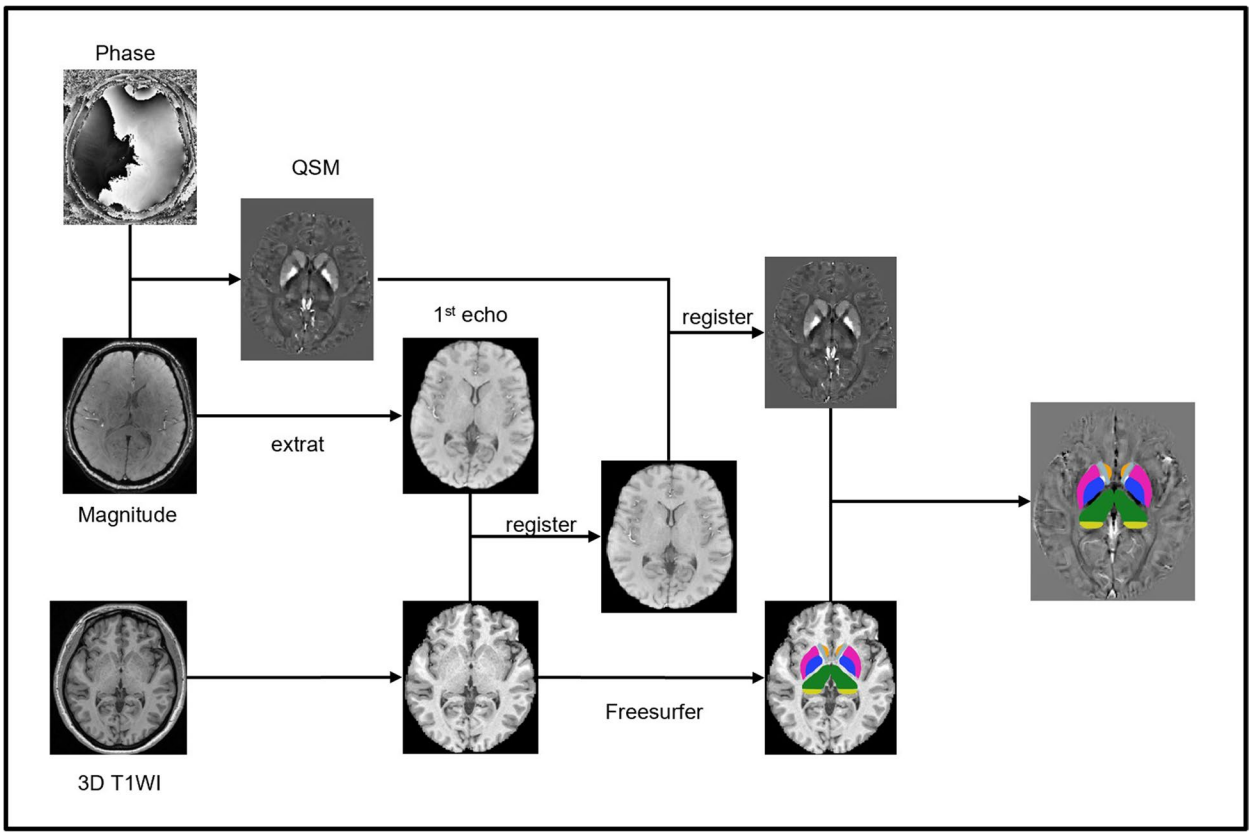

Fig. 2 Pipeline of image processing, including preprocessing of QSM images, segmentation of high-resolution structured images, registration of QSM to T1 and extraction of QSM values

The analysis of differences was performed in comparisons between the HCs group and the entire CM group, as well as between the CM with MOH group versus the CM without MOH group. Separate p-values were calculated for each pairwise comparison, and Bonferroni correction was applied to account for multiple comparisons. Since a total of seven regions were analyzed, the Bonferroni correction factor was set to 7, and each p-value was adjusted by dividing it by 7 to reduce the risk of false positives. A partial correlation analysis with age and gender as control variables was used to investigate the correlation between the clinical information scale and the QSM values in the regions where significant abnormalities occurred. For clinical variables with missing data, we applied a case-wise deletion method to handle the missing values. Prior to Receiver Operating Characteristic (ROC) analysis, logistic regression analysis was used to control for the effects of age and gender. In this model, clinical status was the dependent variable, with the QSM values as the independent variables, and age and gender as covariates. The predicted probabilities from the regression model were calculated, and ROC curves were used to assess the diagnostic performance of these probabilities in distinguishing CM from HC, as well as differentiating CM with MOH from CM without MOH. ROC curves for age and gender were also plotted. An area under the curve (AUC) greater than 0.7 was considered indicative of a reliable diagnostic marker [15]. A p-value of less than 0.050 indicates that the test results are statistically significant.

Results

Demographics and clinical characteristics

After excluding 11 patients due to poor image quality, a total of 69 patients and 48 HCs were included in the analysis (Fig. 3). Table 1 shows the demographic and clinical characteristics of the HCs and patients and Table 2 lists the data on CM patients with and without MOH. In the CM without MOH group, two patients had missing data for clinical scales like PHQ-9, GAD-7, PSQI and MoCA, while in the CM with MOH group, three patients had similar missing data. To maintain the accuracy of the correlation analysis, these five patients were excluded. A significant difference in headache frequency ($p = 0.024$) was observed between CM with MOH and CM without MOH, with all other clinical variables showing comparable distributions (all $p > 0.050$). In this study, we observed that most patients have been using a variety of acute medications over a long term to alleviate headache symptoms. Specifically, non-steroidal anti-inflammatory drugs (NSAIDs) are among the most common choices, accounting for 30.3% of the cases. This is followed by paracetamol (18.2%), combination analgesics (15.2%), and triptans (12.1%). Additionally, some participants indicated they resort to traditional Chinese medicine treatments, with Tou Tong Ning being frequently mentioned (12.1%). More than 30% of patients were taking a

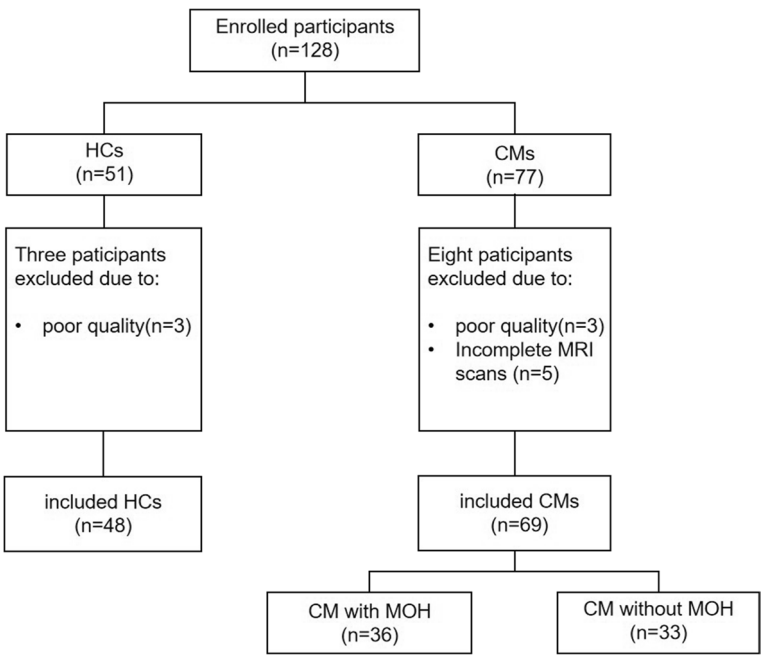

Fig. 3 Flowchart of participant inclusion process

Table 1 Demographic characteristics of HCs and patients

	HCs (*N* = 48)	CM (*N* = 64)	P
Gender (female/male)	30/18	43/21	0.467
Age (years)	38.50 (29.50–49.75)	42.00 (28.50–52.00)	0.388
BMI (kg/m^2)	22.49 (20.20–23.99)	22.29 (20.94–25.18)	0.456
Pain intensity VAS score	NA	7.00 (6.00–8.00)	-
Headache frequency (days/month)	NA	30.00 (17.00–30.00)	-
Headache duration (years)	NA	20.00 (13.00–29.00)	-
MIDAS score	NA	112.00 ± 65.48	-
HIT-6 score	NA	66.00 (64.00–72.00)	-
PHQ-9 score	NA	10.35 ± 6.32	-
GAD-7 scores	NA	6.50 (2.00–12.75)	-
PSQI score	NA	9.86 ± 4.41	-
MoCA score	NA	28.00 (26.00–29.00)	-

Note: Patients with missing data on clinical scales were excluded

Table 2 Demographic characteristics of CM with and without MOH

	CM without MOH (*N* = 31)	CM with MOH (*N* = 33)	P
Gender (female/male)	21/10	22/11	0.813
Age (years)	34.00 (23.00–52.00)	44.00 (33.50–52.50)	0.129
BMI (kg/m^2)	23.11 (21.00–25.51)	21.78 (20.82–24.39)	0.523
Pain intensity VAS score	7.00 (5.75–8.00)	7.00 (6.00–8.75)	0.111
Headache frequency (days/month)	20.00 (15.00–30.00)	30.00 (20.00–30.00)	0.024*
Headache duration (years)	20.34 ± 10.89	22.16 ± 9.48	0.431
MIDAS score	115.70 ± 66.95	108.50 ± 65.22	0.690
HIT-6 score	65.50 (60.50–70.00)	66.50 (63.00–72.25)	0.842
PHQ-9 score	10.76 ± 6.04	9.92 ± 6.79	0.551
GAD-7 scores	6.35 ± 5.81	7.04 ± 6.43	0.421
PSQI score	9.29 ± 4.37	10.20 ± 4.45	0.689
MoCA score	27.00 (25.50–29.00)	28.00 (26.00–30.00)	0.223
Medication Frequency (days/month)	NA	20.00 (15.25–30.00)	-
Duration of medication use (years)	NA	3.00 (1.00–10.00)	-

* Indicates the significant difference ($p < 0.050$)

Note: Patients with missing data on clinical scales were excluded

combination of these medications for more than 10 days per month, with duration ranging from 2 to 20 years.

Comparisons of the QSM values in the DGM among HCs and CM patients with and without MOH

QSM value in the left and right sides of each region were also analyzed in this study. There were no significant differences in QSM values between the left and right sides (Additional File 1: Table S1-S2). Therefore, the values of bilateral sides were put into analysis. Table 3 compares the QSM values in the DGM between the CM patients and HCs and Table 4 shows the difference between the CM patients with and without MOH. Figure 4 illustrates the statistically significant differences in QSM values in the DGM between those groups. Compared to HCs, CM patients as a whole group demonstrated significantly increased iron deposition in the caudate ($p = 0.013$) and putamen ($p < 0.001$). Within the subgroup analysis of CM patients, those with MOH exhibited notably higher QSM values in the caudate ($p < 0.001$), putamen ($p < 0.001$), and GP ($p = 0.049$) compared to CM without MOH patients.

Correlation analysis of QSM values in DGM with significant differences and clinical variables

After correcting for age and gender, QSM values were not significantly correlated with clinical assessment scales in the overall CM cohort. Subsequent correlation analyses were separately performed in the CM with and without

Table 3 QSM values of DGM between HC and CM groups

	HCs (*N* = 48)	CM (*N* = 69)	*P* value	Adjusted *P* Value
Thalamus	−0.0005 ± 0.0031	−0.0006 ± 0.0023	0.172	> 0.999
Caudate	0.0302 (0.0247, 0.0364)	0.0344 (0.0270,0.0426)	0.002**	0.013*
Putamen	0.0266 ± 0.0120	0.0352 ± 0.0173	< 0.001***	< 0.001***
GP	0.0832 (0.0737, 0.0990)	0.0852 (0.0709, 0.1009)	0.973	> 0.999
Hippocampus	−0.0020 ± 0.0024	−0.0019 ± 0.0017	0.826	> 0.999
Amygdala	−0.0085 ± 0.0035	−0.0074 ± 0.0016	0.132	0.924
Accumbens	0.0096 ± 0.0070	0.0098 ± 0.0079	0.670	> 0.999

* Indicates the significant difference ($p < 0.050$)

** indicates the significant difference ($p < 0.010$)

*** indicates the significant difference ($p < 0.001$)

Table 4 QSM values of DGM between CM with and without MOH groups

	CM without MOH (*N* = 33)	CM with MOH (*N* = 36)	*P* value	Adjusted *P* Value
Thalamus	−0.0006 ± 0.0037	−0.0007 ± 0.0045	0.875	> 0.999
Caudate	0.0339 ± 0.0076	0.0369 ± 0.0095	< 0.001***	< 0.001***
Putamen	0.0314 ± 0.0147	0.0387 ± 0.0158	< 0.001***	< 0.001***
GP	0.0821 (0.0690, 0.0979)	0.0868 (0.0720, 0.1066)	0.007**	0.049*
Hippocampus	−0.0018 ± 0.0015	−0.0024 ± 0.0021	0.139	0.976
Amygdala	−0.0085 ± 0.0027	−0.0102 ± 0.0043	0.009**	0.064
Accumbens	0.0110 ± 0.0065	0.0088 ± 0.0076	0.843	> 0.999

* Indicates the significant difference ($p < 0.050$)

** indicates the significant difference ($p < 0.010$)

*** indicates the significant difference ($p < 0.001$)

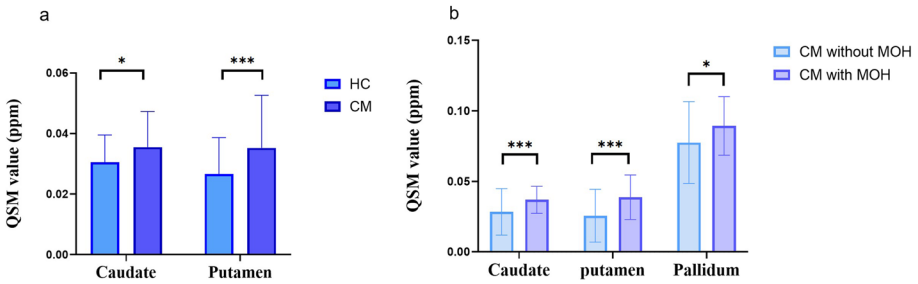

Fig. 4 Comparison of QSM value between those groups (**a**) Comparison of iron deposition between HCs and CM patients, with statistically significant differences in the caudate and putamen. (**b**) Comparison of iron deposition between CM patients with and without MOH, with significant differences in the caudate, putamen and GP. *Indicates the significant difference ($p < 0.050$). ***indicates the significant difference ($p < 0.001$)

MOH cohorts. In CM without MOH patients, QSM values in the caudate (r = 0.502, $p = 0.010$) and putamen (r = 0.514, $p = 0.009$) were significantly correlated with headache duration. Among CM with MOH patients, the QSM values in the caudate (r = 0.400, $p = 0.028$) and putamen (r = 0.475, $p = 0.008$) were significantly correlated with the monthly medication frequency. To further control for the potential influence of headache duration on iron deposition in MOH, a partial correlation analysis was conducted after adjusting for age, gender, and headache duration. The results indicated that the correlation between monthly medication frequency and iron deposition remained significant (caudate: r = 0.427, $p = 0.023$; putamen: r = 0.445, $p = 0.018$) (Fig. 5).

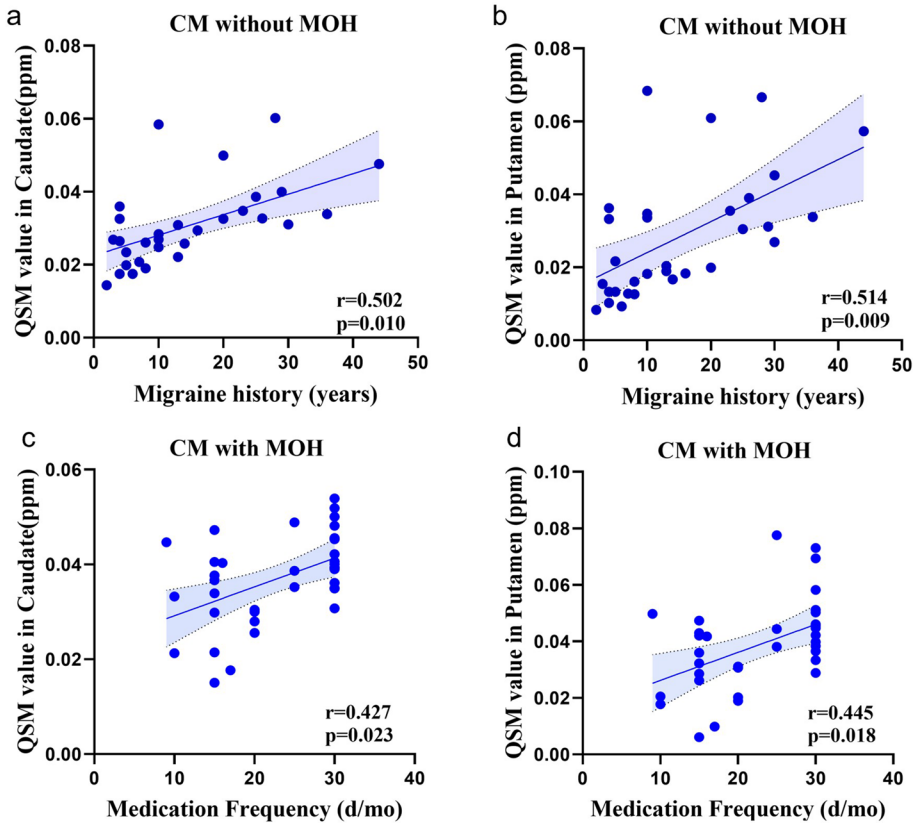

Fig. 5 Correlation analysis of QSM and clinical variables. (**a**, **b**) Correlation between headache duration and iron deposition in the caudate and putamen in the CM group without MOH. (**c**, **d**) Correlation between iron deposition in the caudate and putamen in MOH and the frequency of monthly medication use

ROC Analysis of QSM values in distinguishing CM Patients from HCs and identifying CM with MOH in CM without MOH

As shown in Fig. 6 and Table 5, for discriminating CM from HCs, the AUC for age was 0.505 (95% confidence interval [CI] 0.399–0.611), and for gender was 0.514 (95% CI 0.407–0.620). For distinguishing CM patients with MOH from those without MOH, the AUC for age was 0.644 (95% CI 0.508–0.780), and for gender was 0.513 (95% CI 0.373–0.655). After adjusting for age and gender, the AUCs for the caudate were 0.619 (95% CI 0.518–0.720) and 0.646 (95% CI 0.547–0.746) for putamen in distinguish CM from HC. And the AUCs for the caudate, putamen, and GP were 0.736 (95% CI 0.613–0.859), 0.729 (95% CI 0.605–0.852), and 0.644 (95% CI 0.508–0.780), in distinguish CM with MOH from CM without MOH, respectively.

Discussion

Our results demonstrated that iron deposition in the caudate and putamen was significantly higher in CM patients than HCs. The MOH group exhibited greater iron deposition in the caudate, putamen, and GP than the CM without MOH group. Furthermore, this excessive iron deposition in CM without MOH was significantly correlated with headache duration and in CM with MOH was associated with monthly medication frequency. QSM values in the caudate and putamen had moderate efficacy for diagnosing CM and reliable performance for diagnosing CM with MOH.

CM patients had higher iron deposition in the caudate and putamen than did the HCs. The dorsal striatum (DS) (including the putamen and caudate) plays an important role in multiple functions including pain processing [26]. Previous research has indicated increased iron deposition in the DS among patients with CM compared to those with episodic migraines and HCs, with iron deposition correlating with a greater migraine burden [15, 27]. And we also observed this abnormal iron deposition was significantly correlated with headache duration in the CM without MOH group. In previous studies, it was found that patients with a longer history of migraine had significantly lower T2* values in specific brain regions, including the putamen and caudate [4, 28]. This correlation was

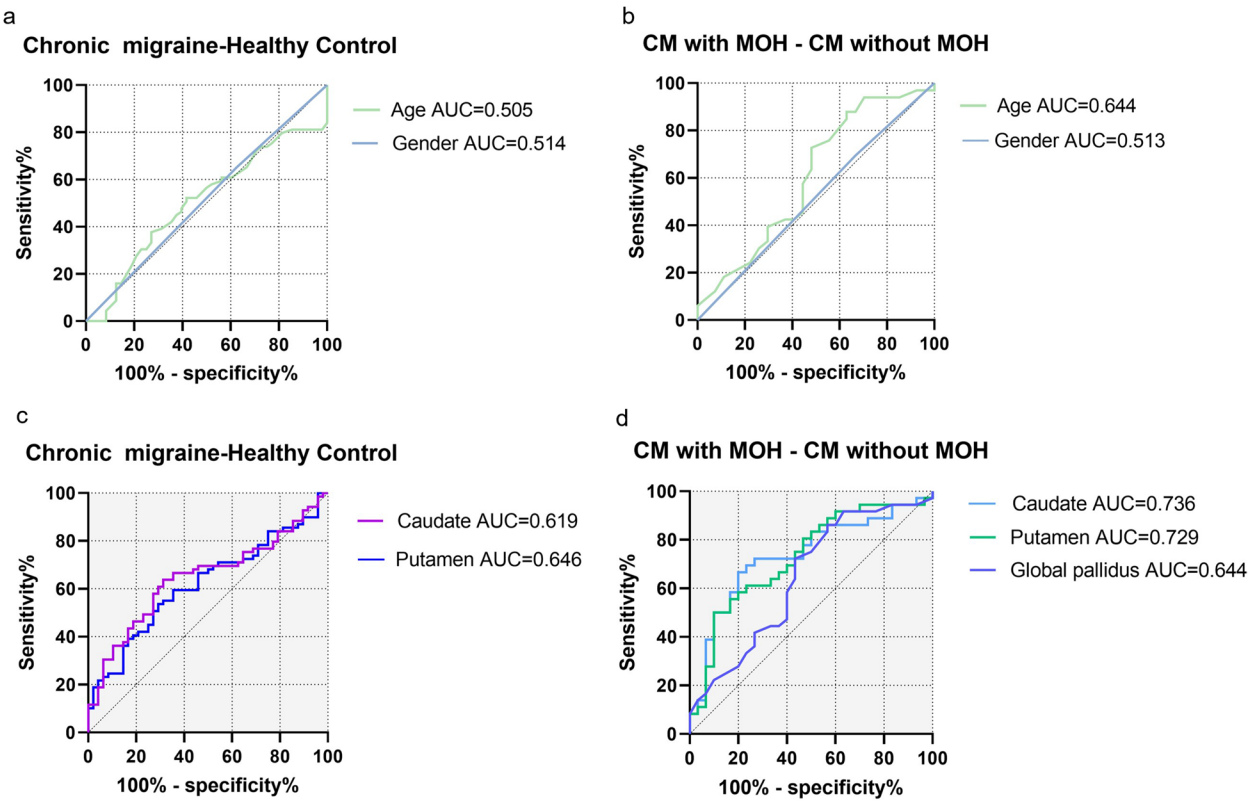

Fig. 6 ROC curves for age, gender and iron deposition. (**a**) ROC curve for the age and gender to diagnose CM from controls. The AUC of age was 0.505 and gender was 0.514. (**b**) ROC curve for the age and gender to diagnose CM from controls. The AUC of age was 0.644 and gender was 0.513. (**c**) After correcting age and gender, ROC curve for the QSM value of Putamen and Caudate to diagnose CM from controls. The AUC of Caudate was 0.619 and Putamen was 0.646. (**d**) After correcting age and gender, ROC curve for the QSM value of Putamen, Caudate and GP diagnose CM with MOH from CM without MOH. The AUC of Caudate was 0.736, Putamen was 0.729 and GP was 0.644

Table 5 ROC analysis results for QSM values to diagnose CM from HCs and diagnose CM with MOH from CM without MOH

	Chronic Migraine—Healthy Controls	CM with MOH—CM without MOH
Caudate		
AUC (95% CI)	0.619 (0.518–0.720)	0.736 (0.613–0.859)
Cut-off value	0.0337	0.0349
Sensitivity (95% CI)	53.62% (41.98% to 64.89%)	66.67% (50.33% to 79.79%)
Specificity (95% CI)	68.75% (54.67% to 80.05%)	80.00% (62.69% to 90.49%)
Putamen		
AUC (95% CI)	0.646 (0.547–0.746)	0.729 (0.605–0.852)
Cut-off value	0.0307	0.0380
Sensitivity (95% CI)	60.87% (49.07% to 71.52%)	55.56% (38.58% to 70.46%)
Specificity (95% CI)	68.75% (54.67% to 80.05%)	83.33% (66.44% to 92.66%)
GP		
AUC (95% CI)	-	0.644 (0.508–0.780)
Cut-off value	-	0.0740
Sensitivity (95% CI)	-	86.11% (71.34% to 93.92%)
Specificity (95% CI)	-	43.33% (27.38% to 60.80%)

The cutoff value was determined using the Youden Index (J = Sensitivity + Specificity—1). The QSM value corresponding to the maximum Youden Index was selected as the cutoff value

particularly evident in migraine patients under the age of fifty, suggesting that patients with a longer headache duration may have more severe iron deposition in these brain areas compared to those with a shorter duration. A plausible explanation may be that recurrent neuroinflammatory episodes and hyperoxia resulting during recurrent migraine attacks make the brain more susceptible to iron-induced oxidative stress [15]. Iron accumulation in the caudate and putamen may be the result of repeated inflammatory responses or changes in brain metabolism associated with chronic pain such as migraine. Therefore, we suggest that iron deposition may serve as a marker for chronic migraine attacks and may indicate a higher headache burden.

In addition, CM with MOH showed significantly greater iron deposition in the caudate, putamen, and GP than did those without MOH. Initially, we speculated that this phenomenon might also be related to the headache burden of the patients, as CM patients with MOH had a markedly elevated headache frequency than those without MOH. However, QSM values were not correlated with headache duration or headache frequency in the CM with MOH group, possibly because the headache frequency in this group already approached a near-saturated level (25 days per month on average). Therefore, detecting correlations in this group may be difficult with such extreme data distributions. This may have also affected the correlation results for the CM group as a whole. But this also raises the question of whether other factors beyond the migraine burden contribute to the presence of abnormal iron deposition in these brain regions during MOH.

In the CM with MOH group, excessive iron deposition was observed in the caudate, putamen, and GP. Additionally, iron deposition in the caudate and putamen correlated with the monthly medication frequency. Iron is an essential element for dopamine synthesis [29] and is critical for participation in the neural mechanisms underlying potential addictive behaviors [30]. Several studies have examined iron deposition changes in individuals with substance overuse. Increased iron deposition in the GP was observed in individuals with cocaine use disorder [31, 32], with similar striatal alterations found in chronic ecstasy users [33]. These alterations can likely be attributed to the neurotoxic effect of excessive medication use, which compromises the integrity of the blood–brain barrier, facilitating iron accumulation [34]. Our findings reveal a correlation between the monthly medication frequency and DS iron deposition, which emphasize the robust association between medication overuse and regional iron accumulation. This interesting finding suggests that MOH patients may experience neurotoxic processes resembling those induced by medication overuse.

The DS and GP are crucial regions involved in reward processing, activated by pleasurable stimuli such as food or anticipation of benefit [35, 36]. These regions receive dopaminergic input at the synapse level and maintain the habit of excessive medication use [37]. Previous research has demonstrated increased volumes in the caudate and putamen in individuals with cocaine use disorder, indicating an association between potential addiction and the DS [38]. Furthermore, neural connectivity from the caudate to the putamen has been also associated with the severity of chronic cocaine use [38]. Studies also indicated a reduced volume in the GP of heroin use disorder [39]. MOH has been proposed to share neurobiological similarities with potential addiction [40]. This association was first suggested by Calabresi and Cupini et al. in 2005 [41] and was later supported by positron emission tomography (PET) studies, which revealed persistent hypometabolism in the orbitofrontal cortex even after drug discontinuation [42]. Further evidence comes from voxel-based morphometry (VBM) studies, which have identified structural abnormalities in the striatum of MOH patients compared to controls and CM patients [43, 44]. Additionally, functional magnetic resonance imaging studies (fMRI) have demonstrated altered connectivity in key regions of the pain-reward system, including the nucleus accumbens, caudate, hippocampus, PAG, precuneus, and insula [45–47]. In this context, the abnormalities in iron deposition observed in the DS and GP may contribute to the mechanisms underlying medication overuse behavior in MOH. Notably, the QSM values in the caudate and putamen demonstrated reliable sensitivity and specificity for identifying MOH within the CM group, with AUC values exceeding 0.7. As for the evaluation of the diagnostic performance, AUC above 0.8 is generally regarded as a strong marker. But previous study has also used AUC of 0.7 as a reliable threshold [15]. Although a higher AUC would provide stronger diagnostic confidence, our findings suggest that the AUC values of 0.729 and 0.736 indicate that excessive iron deposition in the caudate and putamen may serve as a potential imaging biomarker for differentiating CM patients with MOH from those without MOH.

Limitations

This study had several limitations. First, the variability in medications used by patients may have influenced our findings, as we could not fully account for their differential effects on MOH development or iron deposition. Future studies should explore the relationship between specific types of medication and neurotoxic effects. Second, some observed differences, particularly in the GP ($p = 0.049$), had borderline statistical significance and should be interpreted with caution. Third,

the cross-sectional design precludes causal inferences regarding medication overuse and iron accumulation. Additionally, we focused only on iron deposition within the DGM, leaving open the question of potential changes in other brain regions. And the use of a maximum TE of 23.4 ms may also have limited the detection of low susceptibility values in QSM. Finally, while genetic polymorphisms related to serotoninergic transmission (SLC6 A4, 5HT1 A, 5HT2 A), dopaminergic transmission (SLC6 A3, COMT, DBH), medication overuse (ACE, OPRM1, BDNF) [48] have been implicated in MOH risk, their precise role remains unclear. Future research into genetic susceptibility may offer further insights into MOH pathophysiology.

Conclusions

In conclusion, our study highlights increased iron deposition in the caudate and putamen of CM patients, with more pronounced accumulation observed in those with MOH. This finding suggests that iron accumulation in DS may be associated with frequent medication use and further supports the common mechanism between MOH and potential addiction. However, interpretation of these findings requires caution given the study's limitations, including borderline statistical significance in some regions, heterogeneous medication use among participants, and the cross-sectional design that precludes causal inferences. While these QSM findings offer novel insights into the pathophysiology of MOH, their potential clinical utility as biomarkers requires validation through longitudinal studies that systematically consider medication-specific effects. Further studies may help elucidate the complex mechanisms driving the progression from chronic migraine to medication-overuse headache.

Abbreviations

AUC	Area Under the Curve
BET	Brain Extraction Tool
BMI	Body Mass Index
CM	Chronic Migraine
DGM	Deep Gray Matter
DS	Dorsal Striatum
FLIRT	Linear Image Alignment Tool for FMRIB
FMRIB	Functional Magnetic Resonance Imaging of the Brain
fMRI	Functional Magnetic Resonance Imaging
FOV	Field Of View
FSL	FMRIB's Software Library
GAD-7	Generalized Anxiety Disorder-7
GP	Globus Pallidus
GRE	Gradient Recalled Echo
HCs	Healthy Controls
HIT-6	Headache Impact Test-6
ICHD-3	The International Classification of Headache Disorders, 3rd edition
MoCA	Montreal Cognitive Assessment
MOH	Medication-Overuse Headache
MPRAGE	Magnetization-Prepared Rapid Gradient-Echo
MRI	Magnetic Resonance Imaging
MSDI	Multi-Scale Dipole Inversion
NSAIDs	Non-Steroidal Anti-Inflammatory Drugs
PAG	Periaqueductal Gray
PET	Positron Emission Tomography
PHQ-9	Patient Health Questionnaire-9
PSQI	Pittsburgh Sleep Quality Index
QSM	Quantitative Susceptibility Mapping
ROC	Receiver Operating Characteristic
ROI	Regions Of Interest
T1WI	T1-Weighted Image
TE	Echo Time
TR	Repetition Time
VAS	Visual Analog Scale
VBM	Voxel Based Morphometry
95% CI	95% Confidence Interval

Supplementary Information

The online version contains supplementary material available at https://doi.org/10.1186/s12916-025-04125-8.

Supplementary Material 1: Table S1-S2.Table S1 - Left and Right QSM values of DGM in HC and CM groups. Table S2 - Left and Right QSM values of DGM in CM with and without MOH groups

Supplementary Material 2.

Acknowledgements

We sincerely thank all participants for their involvement in this study.

Authors' contributions

XP, QY, YGW and BBS designed the study. XP wrote the first manuscript. YLM, WW and XYZ assisted with patient recruitment. ZYY and PZ collected the clinical data. XYB, XZ, TC and YBZ collected the MRI data. ZXH and YKZ assisted the MRI data pre-processed. HFT, YQZ, XYY and XQJ assisted with research design. All authors contributed to the final manuscript. All authors read and approved the final manuscript.

Funding

This study was supported by the National Natural Science Foundation of China (Grant Nos. 62271061, 32170752, 91849104, and 31770800), the Beijing Municipal Natural Science Foundation (Grant No. L232130), National High Level Hospital Clinical Research Funding (BJ-2025-042) and the National Natural. Science Foundation of Beijing (Z200024).

Data availability

The datasets generated and analysed during the current study are not publicly available due privacy or ethical restrictions but are available from the corresponding author on reasonable request.

Declarations

Ethics approval and consent to participate

All participants received comprehensive details regarding the study and provided written informed consent prior to participation. The study was approved by the Ethics Committee of Beijing Tiantan Hospital, Capital Medical University (Approval No. KY2022-044) and registered at ClinicalTrials.gov (NCT05334927).

Consent for publication

All authors authorize the publication.

Competing interests

The authors declare no competing interests.

Author details

[1]Tiantan Neuroimaging Center for Excellence, China National Clinical Research Center for Neurological Diseases, Beijing Tiantan Hospital, Capital Medical University, Beijing, China. [2]Department of Radiology, Beijing Tiantan Hospital, Capital Medical University, Beijing, China. [3]Headache Center, Department of Neurology, Beijing Tiantan Hospital, Capital Medical University, Beijing, China. [4]Department of Radiology, Beijing Chaoyang Hospital, Capital Medical

UniversityKey Lab of Medical Engineering for Cardiovascular Disease, Ministry of Education, Beijing, China. [5]GE Healthcare, Beijing, China. [6]Department of Radiology, Beijing Hospital, Beijing, China.

Received: 23 June 2024 Accepted: 13 May 2025
Published online: 28 May 2025

References

1. Buse DC, Manack AN, Fanning KM, Serrano D, Reed ML, Turkel CC, et al. Chronic migraine prevalence, disability, and sociodemographic factors: results from the American Migraine Prevalence and Prevention Study. Headache. 2012;52(10):1456–70.
2. Headache Classification Committee of the International Headache Societ y (IHS) The International Classification of Headache Disorders, 3rd ed ition. Cephalalgia. 2018;38(1):1–211.
3. Filippi M, Messina R. The Chronic Migraine Brain: What Have We Learned From Neuroimaging? Front Neurol. 2020;10:1356.
4. Kruit MC, Launer LJ, Overbosch J, van Buchem MA, Ferrari MD. Iron accumulation in deep brain nuclei in migraine: a population-based magnetic resonance imaging study. Cephalalgia. 2009;29(3):351–9.
5. Lai T-H, Wang S-J. Neuroimaging Findings in Patients with Medication Overuse Headache. Curr Pain Headache Rep. 2018;22(1):1.
6. Chen Z, Chen X, Liu M, Dong Z, Ma L, Yu S. Altered functional connectivity architecture of the brain in medicatio n overuse headache using resting state fMRI. J Headache Pain. 2017;18(1):25.
7. Thirupathi A, Chang Y-Z. Brain Iron Metabolism and CNS Diseases. Adv Exp Med Biol. 2019;1173:1–19.
8. Sun C, Wu Y, Ling C, Xie Z, Kong Q, Fang X, et al. Deep Gray Matter Iron Deposition and Its Relationship to Clinical Feat ures in Cerebral Autosomal Dominant Arteriopathy With Subcortical Infa rcts and Leukoencephalopathy Patients: A 7.0-T Magnetic Resonance Imag ing Study. Stroke. 2020;51(6):1750–7.
9. De Lury AD, Bisulca JA, Lee JS, Altaf MD, Coyle PK, Duong TQ. Magnetic resonance imaging detection of deep gray matter iron depositi on in multiple sclerosis: A systematic review. J Neurol Sci. 2023;453:120816.
10. Noseda R, Burstein R. Migraine pathophysiology: anatomy of the trigeminovascular pathway and associated neurological symptoms, CSD, sensitization and modulation o f pain. Pain. 2013;154 Suppl 1:https://doi.org/10.1016/j.pain.2013.07.021.
11. Brennan KC, Pietrobon D. A Systems Neuroscience Approach to Migraine. Neuron. 2018;97(5):1004–21.
12. He M, Kis-Jakab G, Komáromy H, Perlaki G, Orsi G, Bosnyák E, et al. The volume of the thalamus and hippocampus in a right-handed female ep isodic migraine group. Front Neurol. 2023;14:1254628.
13. Bai X, Wang W, Zhang X, Hu Z, Zhang X, Zhang Y, et al. Hyperperfusion of bilateral amygdala in patients with chronic migraine : an arterial spin-labeled magnetic resonance imaging study. J Headache Pain. 2023;24(1):138.
14. Yuan K, Zhao L, Cheng P, Yu D, Zhao L, Dong T, et al. Altered structure and resting-state functional connectivity of the bas al ganglia in migraine patients without aura. J Pain. 2013;14(8):836–44.
15. Xu X, Zhou M, Wu X, Zhao F, Luo X, Li K, et al. Increased iron deposition in nucleus accumbens associated with disease progression and chronicity in migraine. BMC Med. 2023;21(1):136.
16. Guan X, Lancione M, Ayton S, Dusek P, Langkammer C, Zhang M. Neuroimaging of Parkinson's disease by quantitative susceptibility map ping. Neuroimage. 2024;289:120547.
17. Sato R, Kudo K, Udo N, Matsushima M, Yabe I, Yamaguchi A, et al. A diagnostic index based on quantitative susceptibility mapping and vo xel-based morphometry may improve early diagnosis of Alzheimer's disea se. Eur Radiol. 2022;32(7):4479–88.
18. Wang Y, Spincemaille P, Liu Z, Dimov A, Deh K, Li J, et al. Clinical quantitative susceptibility mapping (QSM): Biometal imaging a nd its emerging roles in patient care. J Magn Reson Imaging. 2017;46(4):951–71.
19. Takahashi TT, Ornello R, Quatrosi G, Torrente A, Albanese M, Vigneri S, et al. Medication overuse and drug addiction: a narrative review from addicti on perspective. J Headache Pain. 2021;22(1):32.
20. Vandenbussche N, Laterza D, Lisicki M, Lloyd J, Lupi C, Tischler H, et al. Medication-overuse headache: a widely recognized entity amidst ongoing debate. J Headache Pain. 2018;19(1):50.
21. Acosta-Cabronero J, Milovic C, Mattern H, Tejos C, Speck O, Callaghan MF. A robust multi-scale approach to quantitative susceptibility mapping. Neuroimage. 2018;183:7–24.
22. Pépin J, Francelle L, Carrillo-de Sauvage M-A, de Longprez L, Gipchtein P, Cambon K, et al. In vivo imaging of brain glutamate defects in a knock-in mouse model o f Huntington's disease. Neuroimage. 2016;139:53–64.
23. Fischl B, Salat DH, Busa E, Albert M, Dieterich M, Haselgrove C, et al. Whole brain segmentation: automated labeling of neuroanatomical struct ures in the human brain. Neuron. 2002;33(3):341–55.
24. Jenkinson M, Bannister P, Brady M, Smith S. Improved optimization for the robust and accurate linear registration and motion correction of brain images. Neuroimage. 2002;17(2):825–41.
25. Straub S, Schneider TM, Emmerich J, Freitag MT, Ziener CH, Schlemmer H-P, et al. Suitable reference tissues for quantitative susceptibility mapping of the brain. Magn Reson Med. 2017;78(1):204–14.
26. Boccella S, Marabese I, Guida F, Luongo L, Maione S, Palazzo E. The Modulation of Pain by Metabotropic Glutamate Receptors 7 and 8 in the Dorsal Striatum. Curr Neuropharmacol. 2020;18(1):34–50.
27. Domínguez C, López A, Ramos-Cabrer P, Vieites-Prado A, Pérez-Mato M, Villalba C, et al. Iron deposition in periaqueductal gray matter as a potential biomarker for chronic migraine. Neurology. 2019;92(10):e1076–85.
28. Tepper SJ, Lowe MJ, Beall E, Phillips MD, Liu K, Stillman MJ, et al. Iron deposition in pain-regulatory nuclei in episodic migraine and chronic daily headache by MRI. Headache. 2012;52(2):236–43.
29. Hare DJ, Double KL. Iron and dopamine: a toxic couple. Brain. 2016;139(Pt 4):1026–35.
30. Juhás M, Sun H, Brown MRG, MacKay MB, Mann KF, Sommer WH, et al. Deep grey matter iron accumulation in alcohol use disorder. Neuroimage. 2017;148:115–22.
31. Adisetiyo V, McGill CE, DeVries WH, Jensen JH, Hanlon CA, Helpern JA. Elevated Brain Iron in Cocaine Use Disorder as Indexed by Magnetic Fie ld Correlation Imaging. Biol Psychiatry Cogn Neurosci Neuroimaging. 2019;4(6):579–88.
32. Ersche KD, Acosta-Cabronero J, Jones PS, Ziauddeen H, van Swelm RPL, Laarakkers CMM, et al. Disrupted iron regulation in the brain and periphery in cocaine addict ion. Transl Psychiatry. 2017;7(2):e1040.
33. Coray RC, Berberat J, Zimmermann J, Seifritz E, Stock A-K, Beste C, et al. Striatal Iron Deposition in Recreational MDMA (Ecstasy) Users. Biol Psychiatry Cogn Neurosci Neuroimaging. 2023;8(9):956–66.
34. Yamamoto BK, Raudensky J. The role of oxidative stress, metabolic compromise, and inflammation i n neuronal injury produced by amphetamine-related drugs of abuse. J Neuroimmune Pharmacol. 2008;3(4):203–17.
35. Hong S-I, Kang S, Baker M, Choi D-S. Astrocyte-neuron interaction in the dorsal striatum-pallidal circuits and alcohol-seeking behaviors. Neuropharmacology. 2021;198:108759.
36. Soares-Cunha C, Coimbra B, Sousa N, Rodrigues AJ. Reappraising striatal D1- and D2-neurons in reward and aversion. Neurosci Biobehav Rev. 2016;68:370–86.
37. Lüscher C, Robbins TW, Everitt BJ. The transition to compulsion in addiction. Nat Rev Neurosci. 2020;21(5):247–63.
38. Jacobsen LK, Giedd JN, Gottschalk C, Kosten TR, Krystal JH. Quantitative morphology of the caudate and putamen in patients with cocaine dependence. Am J Psychiatry. 2001;158(3):486–9.
39. Müller UJ, Mawrin C, Frodl T, Dobrowolny H, Busse S, Bernstein H-G, et al. Reduced volumes of the external and internal globus pallidus in male heroin addicts: a postmortem study. Eur Arch Psychiatry Clin Neurosci. 2019;269(3):317–24.
40. Chen W, Li H, Hou X, Jia X. Gray matter alteration in medication overuse headache: a coordinates-b ased activation likelihood estimation meta-analysis. Brain Imaging Behav. 2022;16(5):2307–19.
41. Calabresi P, Cupini LM. Medication-overuse headache: similarities with drug addiction. Trends Pharmacol Sci. 2005;26(2):62–8.
42. Fumal A, Laureys S, Di Clemente L, Boly M, Bohotin V, Vandenheede M, et al. Orbitofrontal cortex involvement in chronic analgesic-overuse headache evolving from episodic migraine. Brain. 2006;129(Pt 2):543–50.
43. Riederer F, Marti M, Luechinger R, Lanzenberger R, von Meyenburg J, Gantenbein AR, et al. Grey matter changes associated with

medication-overuse headache: corre lations with disease related disability and anxiety. World J Biol Psychiatry. 2012;13(7):517–25.
44. Lai T-H, Chou K-H, Fuh J-L, Lee P-L, Kung Y-C, Lin C-P, et al. Gray matter changes related to medication overuse in patients with chr onic migraine. Cephalalgia. 2016;36(14):1324–33.
45. Ferraro S, Grazzi L, Muffatti R, Nava S, Ghielmetti F, Bertolino N, et al. In medication-overuse headache, fMRI shows long-lasting dysfunction in midbrain areas. Headache. 2012;52(10):1520–34.
46. Torta DM, Costa T, Luda E, Barisone MG, Palmisano P, Duca S, et al. Nucleus accumbens functional connectivity discriminates medication-ove ruse headache. Neuroimage Clin. 2016;11:686–93.
47. Chanraud S, Di Scala G, Dilharreguy B, Schoenen J, Allard M, Radat F. Brain functional connectivity and morphology changes in medication-ove ruse headache: Clue for dependence-related processes? Cephalalgia. 2014;34(8):605–15.
48. Cargnin S, Viana M, Sances G, Tassorelli C, Terrazzino S. A systematic review and critical appraisal of gene polymorphism association studies in medication-overuse headache. Cephalalgia. 2018;38(7):1361–73.

Publisher's Note